




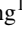
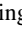
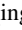


A Robust Multi-View System for High-Fidelity Human Body Shape Reconstruction <Supplementary Material>

Qitong Zhang¹  Lei Wang¹  Linlin Ge¹  Shan Luo¹  Taihao Zhu¹  Feng Jiang¹  Jimmy Ding¹  and Jieqing Feng¹ 

¹State Key Laboratory of CAD&CG, Zhejiang University, China

1. Quantitative Comparisons of Dense Reconstruction

We design a user study to assess the quality of point clouds using 5 different multi-view stereo algorithms. First, we divide 30 reconstructed point clouds, which are from 5 subjects and 6 fixed parts, into two groups including 16 and 14 point clouds that are seriously and weakly impacted by body hair. Then, 24 volunteers, with ages ranging from 22 to 33 years old (the mean is 25) and sufficient relevant knowledge of computer graphics and computer vision, are recruited to score the point clouds by their qualities (decreasing from 5 to 1). An example of human body shape, which is acquired by a high-end active-vision system and included in the FAUST dataset [BRLB14], and the source images are offered for quality reference. The instruction and question are shown as follows:

1. “These point clouds were reconstructed using 5 different algorithms from the source images.”
2. “According to the given high-quality point cloud example, the source images, and your understanding of high quality, please firstly sort these point clouds by their qualities and then score them from 5 to 1 in order. (The higher, the better.)”

The example is randomly picked from the dataset and shown in Figure 1.

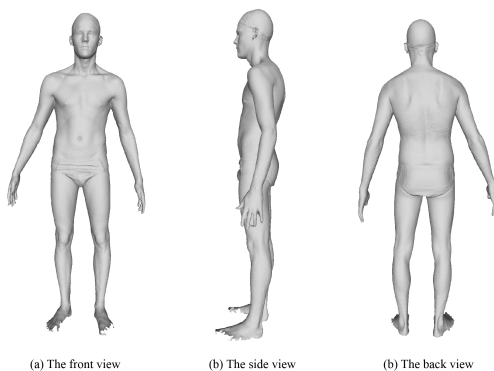


Figure 1: The example of scanned human body shape point cloud from FAUST dataset [BRLB14].

The mean score (M) and standard deviation (Std) of each part are

given in Table 1. We denote the 6 parts including the back, breast, abdomen, arm, thigh, and calf as Ba, Br, Ab, Ar, Th, and Ca, respectively. The number followed by the abbreviation of the 6 parts is the number of the subject. The 5 different algorithms include OpenMVS [cdc], COLMAP [SZFP16], our method without the local smoothness constraint (w/o SC), our method without the hierarchical framework (w/o HF), and our method. It can be found that our method performs best in almost all parts of the reconstructed point clouds.

Table 1: Quantitative point cloud comparisons using different MVS methods.

	Parts	OpenMVS		COLMAP		w/o SC		w/o HF		Ours	
		M	Std	M	Std	M	Std	M	Std	M	Std
SIR	Br1	2.79	1.04	1.25	0.52	3.88	0.73	2.25	0.52	4.63	0.90
	Ab1	3.04	1.17	1.29	0.73	3.54	0.87	2.46	0.71	4.58	0.81
	Ar1	1.21	0.50	1.88	0.67	3.58	0.64	3.13	0.78	4.92	0.40
	Th1	3.33	0.75	1.00	0.00	3.46	0.58	2.09	0.28	4.92	0.40
	Ca1	3.83	1.03	1.04	0.20	3.63	0.48	2.04	0.20	4.5	0.76
	Ab3	2.50	1.00	1.33	0.62	2.88	0.97	3.42	0.86	4.71	0.89
	Ar3	1.00	0.00	2.25	0.60	2.96	0.61	3.92	0.86	4.67	0.55
	Th3	2.04	1.06	1.96	0.89	3.88	0.44	2.00	0.76	4.88	0.44
	Ca3	2.92	0.95	1.13	0.33	3.46	0.58	2.25	0.78	4.92	0.40
	Th4	2.92	1.11	1.63	0.81	3.50	0.58	2.04	0.84	4.79	0.82
	Ca4	4.42	0.64	1.88	0.73	1.42	0.70	2.71	0.61	4.33	0.62
	Ba5	1.00	0.00	2.08	0.40	4.08	0.64	2.96	0.45	4.63	0.63
	Br5	1.00	0.00	2.38	0.63	4.00	0.29	2.92	0.64	4.79	0.64
	Ab5	1.00	0.00	2.17	0.37	4.04	0.79	3.00	0.58	4.54	0.87
	Th5	1.29	0.68	1.92	0.64	3.67	0.80	3.00	0.50	4.92	0.28
	Ca5	1.50	0.91	1.63	0.48	3.83	0.37	2.96	0.45	4.92	0.28
Avr	2.24	1.36	1.67	0.73	3.49	0.91	2.70	0.84	4.73	0.67	
WIR	Ba1	1.25	0.52	2.17	0.94	3.75	0.83	3.21	0.82	4.75	0.52
	Ba2	1.88	1.40	4.13	0.53	2.21	0.76	3.13	0.88	4.38	1.18
	Br2	2.42	1.04	3.33	1.43	2.63	1.35	2.79	1.04	4.38	0.99
	Ab2	1.46	0.82	2.83	1.21	3.54	1.32	3.54	1.00	3.79	1.08
	Ar2	1.08	0.40	2.83	0.55	2.42	0.64	4.00	0.29	4.96	0.20
	Th2	1.88	1.30	1.96	0.68	3.83	0.90	2.63	0.56	4.88	0.33
	Ca2	3.96	1.49	1.71	0.68	3.42	1.22	2.00	1.00	4.00	0.82
	Ba3	1.29	0.68	2.38	0.86	3.21	0.91	3.33	0.90	4.88	0.44
	Br3	1.67	0.80	1.83	0.85	4.00	0.41	2.75	0.83	4.79	0.64
	Ba4	1.42	0.81	3.04	1.40	3.75	0.78	3.33	1.14	4.04	0.98
	Ab4	1.75	1.13	3.21	1.32	3.42	1.44	3.21	0.87	3.29	1.46
	Br4	2.04	1.06	2.25	1.30	4.04	0.73	2.58	0.86	4.42	0.91
	Ar4	3.96	0.93	2.25	0.88	1.58	1.04	2.96	0.73	4.25	1.20
	Th5	1.04	0.20	2.21	0.50	3.21	0.76	3.67	0.75	4.79	0.50
	Avr	1.93	1.32	2.58	1.19	3.21	1.21	3.08	0.99	4.40	1.00

2. High-Fidelity Human Body Shape Dataset

We capture 57 subjects with different genders, poses, and skin with different amounts of body hair, and construct a high-fidelity human body shape dataset consisted of 227 watertight meshes. All the results are shown in Figures 2 and 3. The robustness and accuracy of the proposed system can be demonstrated.

References

- [BRLB14] BOGO F., ROMERO J., LOPER M., BLACK M. J.: FAUST: dataset and evaluation for 3d mesh registration. In *Proc. CVPR '14* (2014), pp. 3794–3801. doi:10.1109/CVPR.2014.491. 1
- [cdc] Openmvs. <https://github.com/cdcseacave/openMVS>. 1
- [SZFP16] SCHÖNBERGER J. L., ZHENG E., FRAHM J., POLLEFEYS M.: Pixelwise view selection for unstructured multi-view stereo. In *Proc. ECCV '16* (2016), vol. 9907, pp. 501–518. doi:10.1007/978-3-319-46487-9_31. 1

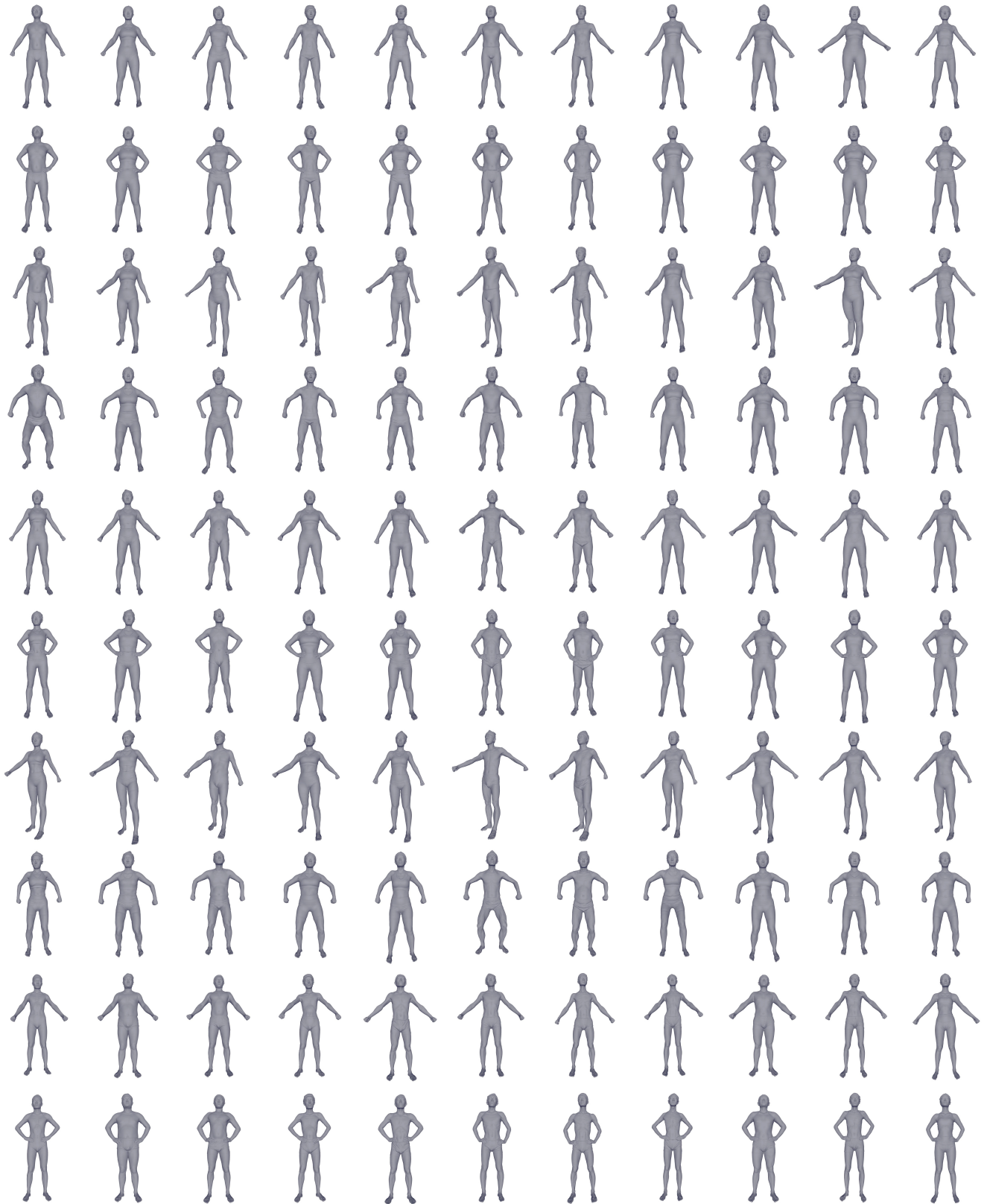


Figure 2: Partially reconstructed results of the human body shape dataset.

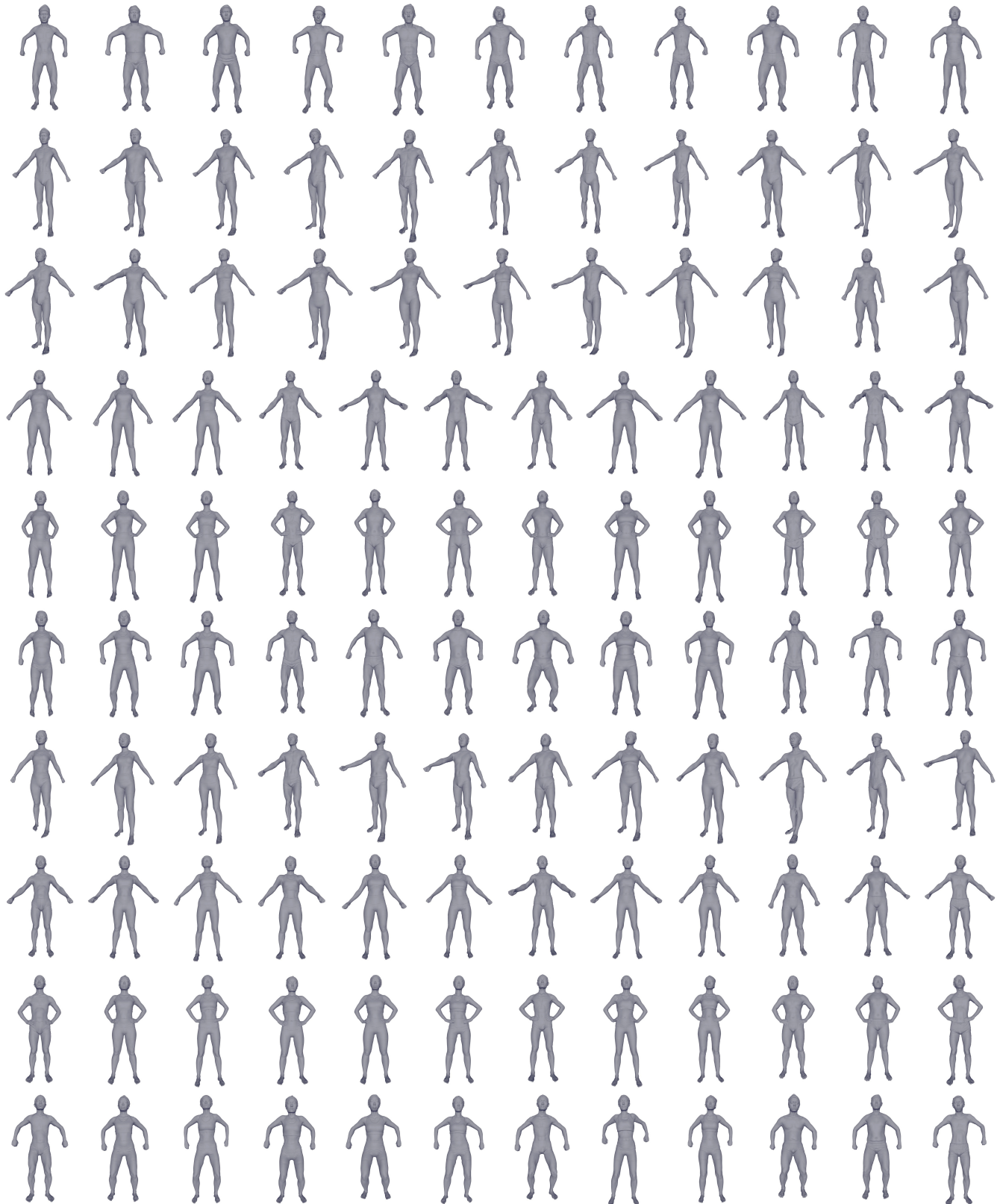


Figure 3: Partially reconstructed results of the human body shape dataset.